Valley mixing in short-period superlattices and the interface matrix

T. Ando
Institute for Solid State Physics, University of Tokyo, 7-22-1 Roppongi, Minato-ku, Tokyo 106, Japan
(Received 9 November 1992)

Energy levels of short-period GaAs/AlAs superlattices are calculated both in an *sps** tight-binding model and in an effective-mass approximation. Mixing between Γ and X conduction-band valleys is shown to be successfully described by a current-conserving interface matrix giving boundary conditions among envelope functions and their derivatives at a heterointerface. Two parameters characterizing the mixing are determined.

I. INTRODUCTION

A typical semiconductor superlattice is that made from GaAs/Al_xGa_{1-x}As heterostructures. The conduction band of GaAs has two local minima along the [001] direction in the vicinity of the X points (called X valleys) as well as the minimum at the Γ point called the Γ valley. On the other hand, AlAs has the lowest minima at the X valleys. At heterointerfaces grown in the [001] direction, these different valleys can be coupled to each other. In a previous paper,[1] the effective-mass approximation was extended so as to take into account the intervalley mixing at heterointerfaces. The purpose of the present paper is to determine effective-mass parameters, which characterize the intervalley mixing, through a comparison of energy levels of short-period superlattices calculated in an *sps** tight-binding model.

In a GaAs/AlAs system the AlAs layer works as a quantum well for the X valley, while the energy of the GaAs layer is lower for the Γ valley. Because the effective mass of the Γ valley is smaller than that of the X valleys, electrons in the Γ valley are raised higher in energy in comparison with those in X valleys for superlattices with sufficiently thin GaAs layers. This leads to a sudden change of the conduction-band bottom from the character of the Γ valley in GaAs to that of X valleys in AlAs (transition from a direct to spatially indirect semiconductor). Numerous optical experiments and band-structure calculations have been performed to understand this crossover with decreasing superlattice period.[2]

Within the effective-mass approximation, mixing of different valleys can be incorporated as boundary conditions for envelope functions at the interface expressed in terms of a 6×6 interface matrix. In a previous paper,[1] this interface matrix was obtained by direct matching of the wave function expressed in terms of envelope functions of different conduction-band minima. Unfortunately, this led to the severe difficulty of violation of flux conservation at the heterointerface. In this paper, the interface matrix is determined by a direct comparison of wave functions in GaAs/AlAs short-period superlattices in such a way that the flux is conserved at the interface.

The paper is organized as follows. In Sec. II the model and the method of calculations are discussed together with a brief review of some properties of the 6×6 interface matrix. Mixing between different valleys is shown to be described by two off-diagonal elements of the interface matrix. In Sec. III the parameters of the interface matrix are determined by a comparison between the wave functions calculated in the tight-binding approximation and the effective-mass approximation. A brief summary is given in Sec. IV.

II. INTERFACE MATRIX

Let us consider a GaAs/Al_xGa_{1-x}As heterointerface grown in the [001] direction. Throughout this paper we confine ourselves to the case $k_x \approx k_y \approx 0$, i.e., along the Δ axis. For the Γ valley we use the conventional envelope $\zeta_\Gamma(z)$ satisfying a single-valley effective-mass equation characterized by an effective mass m_Γ. For X valleys we shall use a 2×2 multicomponent effective-mass equation because of the presence of two bands denoted u (conventionally X_1) and v (X_3) at the X point close to each other in energy. The effective-mass equation in the presence of the external potential $V(z)$ is given by

$$\begin{bmatrix} E_u+V(z)-\dfrac{\hbar^2}{2m_u}\dfrac{d^2}{dz^2} & i\dfrac{\hbar^2P}{2m_0a}\dfrac{d}{idz} \\ -i\dfrac{\hbar^2P}{2m_0a}\dfrac{d}{idz} & E_v+V(z)-\dfrac{\hbar^2}{2m_v}\dfrac{d^2}{dz^2} \end{bmatrix} \begin{bmatrix} \zeta_u \\ \zeta_v \end{bmatrix} = E \begin{bmatrix} \zeta_u \\ \zeta_v \end{bmatrix}, \quad (2.1)$$

where E_u and E_v are the band energies at the X point, m_u and m_v are the effective masses, m_0 is the free-electron mass, and P is the momentum matrix element between u and v.

The presence of abrupt interface potentials gives rise to mixing between three different valleys, $\alpha=\Gamma$, u, and v. Such mixing can be included in the form of a 6×6 interface matrix $T_{BA}=(T_{BA}^{\beta\alpha})$ as follows:

$$\begin{bmatrix} \zeta_\beta^B(0) \\ \nabla_\beta^B\zeta_\beta^B(0) \end{bmatrix} = \sum_\alpha T_{BA}^{\beta\alpha} \begin{bmatrix} \zeta_\alpha^A(0) \\ \nabla_\alpha^A\zeta_\alpha^A(0) \end{bmatrix}, \quad (2.2)$$

where $T_{BA}^{\beta\alpha}=(t_{ij}^{\beta\alpha})$ is a 2×2 matrix; $\nabla_\alpha^A=(m_0/m_\alpha^A)\nabla$; $\nabla_\beta^B=(m_0/m_\beta^B)\nabla$ with m_0 the free-electron mass and m_α^A

and m_α^B the effective masses in semiconductors A and B, respectively, at minimum α; and $\nabla = \partial/a\partial z$, a is the lattice constant. Note that, for simplicity, we shall use $T_{BA}^{\beta\alpha}$ instead of $\tilde{T}_{BA}^{\beta\alpha}$ used in previous papers.[3,1]

Within the *sps** tight-binding model discussed in Ref. 1, the wave function can be represented by the corresponding envelope functions through

$$\mathbf{C}_0(n) = \sum_\alpha \exp(ik_\alpha z_n^0)[\mathbf{C}_0(k_\alpha)\zeta_\alpha(z_n^0) + \mathbf{C}_0'(k_\alpha)\nabla\zeta_\alpha(z_n^0)] , \tag{2.3}$$

$$\mathbf{C}_1(n) = \sum_\alpha \exp(ik_\alpha z_n^1)[\mathbf{C}_1(k_\alpha)\zeta_\alpha(z_n^1) + \mathbf{C}_1'(k_\alpha)\nabla\zeta_\alpha(z_n^1)] ,$$

where $\mathbf{C}_1(n)$ is a vector consisting of the amplitude of cation (Ga or Al) orbitals s_1, p_1, and s_1^* at $z_n^1 = (n - \frac{1}{2})a/2$; $\mathbf{C}_0(n)$ is a vector consisting of the amplitude of anion (As) orbitals s_0, p_0, and s_0^* at $z_n^0 = na/2$; $\mathbf{C}_1(k_\alpha)$ and $\mathbf{C}_0(k_\alpha)$ are the eigenvectors at the valley k_α; and $\mathbf{C}_1'(k_\alpha)$ and $\mathbf{C}_0'(k_\alpha)$ are their first derivative with respect to $k_z a$. We have chosen $z = 0$ at one As atomic plane.

Figure 1 shows the conduction band of GaAs and AlAs in the vicinity of the Γ and X point calculated in the *sps** tight-binding model. The minimum point is slightly displaced (by $k_{\min}$) from the X point for both GaAs and AlAs in this model. The effective masses and the parameter P obtained are listed in Table I. Because of large $k_{\min}$, the straightforward use of the 2×2 effective-mass equation predicts $k_{\min}$ slightly larger than that calculated in the tight-binding model. Therefore, the parameters for the X valleys are modified in such a way that the overall k dependence is reproduced. The bands assumed in the effective-mass approximation are given in Fig. 2 and the corresponding parameters are listed in Table I. The large nonparabolicity of the Γ valley is not so important in the energy range corresponding to the X-valley minimum of AlAs (see below for the choice of the band offset).

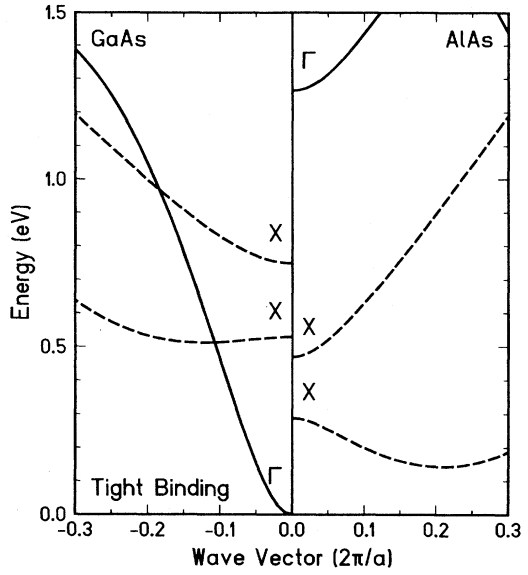

FIG. 1. Energy of the conduction bands calculated in the empirical tight-binding model as a function of the wave vector measured from the Γ point (solid lines) and an X point (dashed lines) for GaAs (left) and AlAs (right). The energy is measured from the bottom of the Γ valley of GaAs.

A matching of the wave functions in an empirical *sps** tight-binding model as in the previous paper gives the following result for the GaAs/AlAs interface:

$$T(\text{AlAs}\leftarrow\text{GaAs}) = \begin{array}{c} \\ \zeta_\Gamma \\ \nabla\zeta_\Gamma \\ \zeta_u \\ \nabla\zeta_u \\ \zeta_v \\ \nabla\zeta_v \end{array} \begin{array}{c} \begin{array}{cccccc} \zeta_\Gamma & \nabla\zeta_\Gamma & \zeta_u & \nabla\zeta_u & \zeta_v & \nabla\zeta_v \end{array} \\ \begin{bmatrix} 1.23 & 0 & -0.05 & 0 & 0 & -0.02 \\ 0 & 0.79 & 0 & 0.09 & -1.03 & 0 \\ 0.00 & 0 & 0.91 & 0 & 0 & -0.01 \\ 0 & 0.00 & 0 & 0.96 & 0.19 & 0 \\ 0 & 0.03 & 0 & -0.03 & 0.81 & 0 \\ 1.10 & 0 & -0.35 & 0 & 0 & 1.20 \end{bmatrix} \end{array} , \tag{2.4}$$

TABLE I. The band parameters used in the energy-band calculation. $k_{\min}$ is the distance of an X-valley minimum from the X point and m_0 is the free-electron mass. The number in parentheses for $k_{\min}$ gives the value obtained by a straightforward use of the parameters in the effective-mass approximation.

GaAs	m_Γ/m_0	m_u/m_0	m_v/m_0	P	$ak_{\min}/2\pi$
Tight binding	0.068	1.35	1.57	1.59	0.123 (0.154)
Effective mass	0.068	1.35	1.57	1.40	0.116
AlAs	m_Γ/m_0	m_u/m_0	m_v/m_0	P	$ak_{\min}/2\pi$
Tight binding	0.222	1.58	1.12	2.69	0.209 (0.275)
Effective mass	0.222	1.00	1.00	2.70	0.210

where the phase of the basis Bloch function is given by Eqs. (2.6) and (2.7) of Ref. 1. Unfortunately, however, this interface matrix violates the current or flux conservation at the interface. It can immediately be seen that the off-diagonal elements of the interface matrix are negligible except for $t_{21}^{\Gamma v}$, $t_{21}^{v\Gamma}$, t_{21}^{uv}, and t_{21}^{vu}. In the effective-mass approximation, the envelope function varies slowly over a distance of the size of a unit cell and therefore the derivative $\nabla\zeta$ is much smaller than the envelope itself. Thus, t_{21} connecting $\nabla\zeta$ and ζ is most important among various elements of the interface matrix unless its absolute value is much smaller than unity. Therefore, it is reasonable to replace the interface matrix by the following approximate expression:

$$T_{BA}=\begin{pmatrix} t_{11}^{\Gamma} & 0 & 0 & 0 & 0 & 0 \\ 0 & t_{22}^{\Gamma} & 0 & 0 & t_{21}^{\Gamma v} & 0 \\ 0 & 0 & t_{11}^{u} & 0 & 0 & 0 \\ 0 & 0 & 0 & t_{22}^{u} & t_{21}^{uv} & 0 \\ 0 & 0 & 0 & 0 & t_{11}^{v} & 0 \\ t_{21}^{v\Gamma} & 0 & t_{21}^{vu} & 0 & 0 & t_{22}^{v} \end{pmatrix} . \tag{2.5}$$

In the following, we shall determine the elements in such a way that they are close to the above equation under the condition of flux conservation.

Now, the current conservation given by Eq. (2.13) of Ref. 1 leads to the relation

$$t_{11}^{\Gamma}t_{22}^{\Gamma}=1 , \tag{2.6a}$$

$$t_{11}^{u}t_{22}^{u}=1 , \tag{2.6b}$$

$$t_{11}^{v}t_{22}^{v}=1 , \tag{2.6c}$$

$$t_{11}^{\Gamma}t_{21}^{\Gamma v}-t_{11}^{v}t_{21}^{v\Gamma}=0 , \tag{2.6d}$$

$$t_{11}^{u}t_{21}^{uv}-t_{11}^{v}t_{21}^{vu}=t_{11}^{u}t_{11}^{v}P_B-P_A . \tag{2.6e}$$

These conditions are satisfied within a reasonable accuracy, except Eq. (2.6d) for $t_{21}^{\Gamma v}$ and $t_{21}^{v\Gamma}$. It is this large deviation from (2.6d) that makes a unique determination of these two most important parameters leading to the Γ-X mixing impossible. Therefore, we shall assume

$$t_{21}^{\Gamma v}=-t_{11}^{v}p \text{ and } t_{21}^{v\Gamma}=-t_{11}^{\Gamma}p , \tag{2.7}$$

which satisfies Eq. (2.6d), and try to determine the parameter p through a direct comparison of wave functions calculated in the effective-mass approximation and in the tight-binding model in short-period superlattices. Note that the sign of p depends on the choice in the relative phase of the Bloch wave functions at Γ and X and therefore will be chosen to be positive here.

The other parameters are easily determined by a least-squares fit. First, for the current-conserving matrix we have

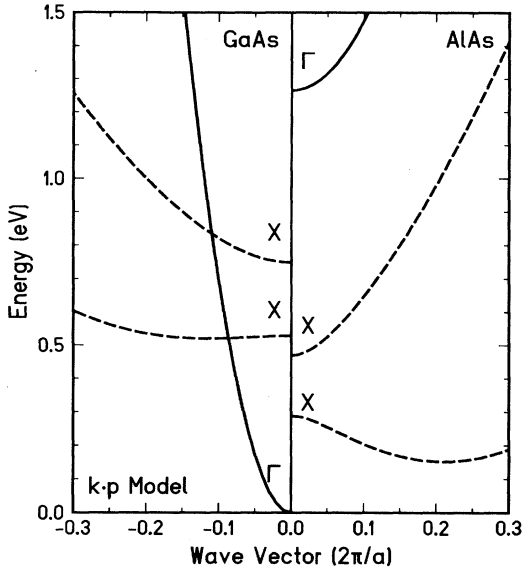

FIG. 2. Energy of the conduction bands assumed in the effective-mass approximation. The notation is the same as in Fig. 1.

$$T_{AB}=T_{BA}^{-1}=\begin{pmatrix} t_{22}^{\Gamma} & 0 & 0 & 0 & 0 & 0 \\ 0 & t_{11}^{\Gamma} & 0 & 0 & -t_{11}^{\Gamma}t_{22}^{v}t_{21}^{\Gamma v} & 0 \\ 0 & 0 & t_{22}^{u} & 0 & 0 & 0 \\ 0 & 0 & 0 & t_{11}^{u} & -t_{11}^{u}t_{22}^{v}t_{21}^{uv} & 0 \\ 0 & 0 & 0 & 0 & t_{22}^{v} & 0 \\ -t_{22}^{\Gamma}t_{11}^{v}t_{21}^{v\Gamma} & 0 & -t_{22}^{u}t_{11}^{v}t_{21}^{vu} & 0 & 0 & t_{11}^{v} \end{pmatrix} . \tag{2.8}$$

We determine the diagonal elements t_{11} and t_{22} by minimizing

$$f(t_{11},t_{22})=(t_{11}^{BA}-t_{11})^2+(t_{22}^{BA}-t_{22})^2+(t_{22}^{AB}-t_{11})^2+(t_{11}^{AB}-t_{22})^2 \tag{2.9}$$

under the condition of current conservation [Eqs. (2.6a)–(2.6c)] for each of the Γ, u, and v valleys, where t_{11}^{AB}, t_{11}^{BA}, etc., are the results obtained by the direct matching given by Eq. (2.4). Similarly, t_{21}^{uv} and t_{21}^{vu} are determined by the minimization of

$$g(t_{21}^{uv},t_{21}^{vu})=(t_{uv}^{BA}-t_{21}^{uv})^2+(t_{uv}^{AB}+t_{11}^{u}t_{22}^{v}t_{21}^{uv})^2+(t_{vu}^{BA}-t_{21}^{vu})^2+(t_{vu}^{AB}-t_{22}^{u}t_{11}^{v}t_{21}^{vu})^2 , \tag{2.10}$$

under the condition given by Eq. (2.6e), where $t_{uv}^{BA}=t_{21}^{vu}$ for T_{BA}, etc. The result is given by

$$T(\text{AlAs}\leftarrow\text{GaAs})=\begin{pmatrix} 1.24 & 0 & 0.00 & 0 & 0 & 0.00 \\ 0 & 0.81 & 0 & 0.00 & -0.83p & 0 \\ 0.00 & 0 & 0.97 & 0 & 0 & 0.00 \\ 0 & 0.00 & 0 & 1.03 & 0.26 & 0 \\ 0 & 0.00 & 0 & 0.00 & 0.83 & 0 \\ -1.24p & 0 & -0.40 & 0 & 0 & 1.20 \end{pmatrix}, \tag{2.11}$$

which is close to Eq. (2.4) except for the elements containing the mixing parameter p. Note that the slightly larger difference for t_{21}^{uv} and t_{21}^{vu} between Eqs. (2.4) and (2.11) is a result of the change in the band parameters in the effective-mass approximation.

The conduction-band bottom of GaAs consists essentially of (antibonding) s states of Ga and As atoms apart from contributions from their s^* atomic orbitals. The X-valley minimum u consists of an antibonding combination of the p_z orbital of Ga and the s orbital of Al. Similarly, the minimum v consists of that of s of Ga and p_z of Al. The most important contribution to the mixing between the Γ and X valleys comes from the p_z state of interfacial Al atoms which belong to both GaAs and AlAs layers. The wave function associated with the v valley leads to an appreciable amplitude of the p_z orbital of the interfacial Al plane. Because the p_z state of Al constitutes a major part of the valence-band top of GaAs and AlAs at the Γ point, this affects the conduction-band envelope function through the interband $\mathbf{k}\cdot\mathbf{p}$ interaction as the source of a discontinuity of its derivative. The resulting parameters $t_{21}^{\Gamma v}$ and $t_{21}^{v\Gamma}$ roughly correspond to an introduction of a δ-function-like potential connecting only Γ- and X-valley envelopes at the heterointerface as postulated previously for a model of Γ-X mixing.[4–6]

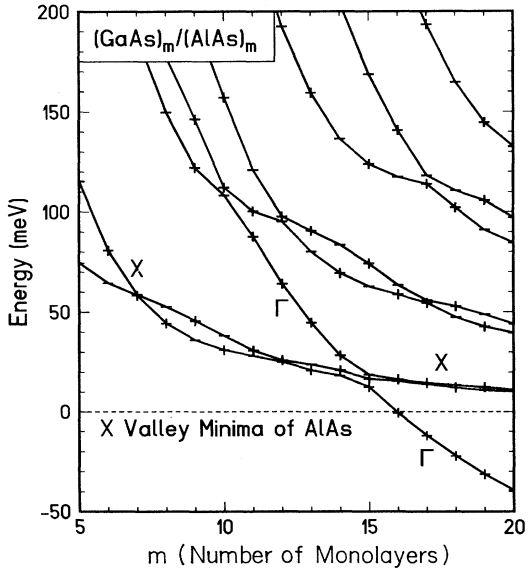

FIG. 3. Energy bands at the Γ point calculated in the empirical tight-binding model of $(\text{GaAs})_m(\text{AlAs})_m$ superlattices as a function of m. The parity of each state is denoted by $+$ and $-$. The energy is measured from the bottom of the conduction-band minimum near the X point.

III. SHORT-PERIOD SUPERLATTICES

In the following band-structure calculation, the difference in the Γ-valley minimum of GaAs and the X-valley minima of AlAs is chosen in such a way that the crossover between Γ and X is around $14 \lesssim m \lesssim 15$ for $(\text{GaAs})_m(\text{AlAs})_m$ superlattices.[7,8] It should be noted that the sign of the Γ-X off-diagonal elements of the interface matrix $t_{21}^{\Gamma v}$ and $t_{21}^{v\Gamma}$ should be changed between two different interfaces for odd m.[9] This arises from the fact that the X-valley Bloch function changes its sign by each monolayer. This leads to a characteristic dependence of the parity of the resulting wave function on m. The present effective-mass scheme is not applicable to $(\text{GaAs})_n(\text{AlAs})_m$ superlattices with odd $m+n$ for which the bulk X point does not coincide with the Γ point after a Brillouin-zone folding.

Figure 3 shows the energy levels at the Γ point of $(\text{GaAs})_m(\text{AlAs})_m$ superlattices as a function of m calculated in the empirical tight-binding model. Figure 4 gives the corresponding results calculated in the effective-mass approximation with the mixing parameter $p=0.5$. As long as p is not so large, the energy levels are nearly in-

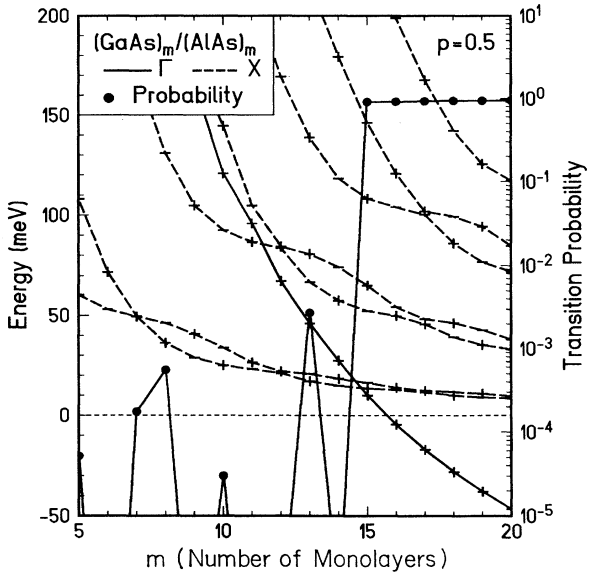

FIG. 4. Energy bands at the Γ point calculated in the effective-mass approximation of $(\text{GaAs})_m(\text{AlAs})_m$ superlattices as a function of m. The parity of each state is denoted by $+$ and $-$. The optical transition probability determined by the overlap of the wave function of the lowest energy level with that of the valence-band top is denoted by filled circles. The energy is measured from the bottom of the conduction-band minimum near the X point.

dependent of p except in the case that those associated with the Γ and X valleys are nearly degenerate with each other. In the present model the X valley has double minima and the presence of interfaces leads to a splitting of the valley degeneracy. This valley splitting exhibits a characteristic oscillatory dependence on m. The effective-mass approximation can reproduce the tight-binding result for the low-lying energy bands including the valley splitting. There appears to be, however, some difference between the results for excited bands.

The valley splitting can easily be estimated in the effective-mass approximation. The Hamiltonian is written as

$$\mathcal{H}=\begin{bmatrix} \frac{\hbar^2k^2}{2m}-\frac{\Delta}{2} & i\frac{\hbar^2Pk}{2m} \\ -i\frac{\hbar^2Pk}{2m} & \frac{\hbar^2k^2}{2m}+\frac{\Delta}{2} \end{bmatrix}, \tag{3.1}$$

where $\Delta=E_v-E_u$ and $m=m_u=m_v$. By a unitary transformation, this can be converted into

$$U^{-1}\mathcal{H}U=\begin{bmatrix} \frac{\hbar^2}{2m}[(k-k_{\min})^2-k_{\min}^2] & -\frac{\Delta}{2} \\ -\frac{\Delta}{2} & \frac{\hbar^2}{2m}[(k+k_{\min})^2-k_{\min}^2] \end{bmatrix} \tag{3.2}$$

with $k_{\min}=P/2$ and

$$U=\begin{bmatrix} 1/\sqrt{2} & 1/\sqrt{2} \\ i/\sqrt{2} & -i/\sqrt{2} \end{bmatrix}. \tag{3.3}$$

Therefore, to the lowest order in Δ the wave function of the minima at $k=\pm k_{\min}$ is given by

$$\begin{aligned} \zeta_+(z)&=\left[\frac{2}{L_W}\right]^{1/2}\exp(+ik_{\min}z)\cos\frac{\pi z}{L_w}\begin{bmatrix}1\\0\end{bmatrix}, \\ \zeta_-(z)&=\left[\frac{2}{L_W}\right]^{1/2}\exp(-ik_{\min}z)\cos\frac{\pi z}{L_w}\begin{bmatrix}0\\1\end{bmatrix}, \end{aligned} \tag{3.4}$$

where we have assumed that electrons are confined by infinitely high walls within $-L_W/2<z<L_W/2$. The splitting is estimated as

$$\left|\int_{-L_W/2}^{L_W/2}\zeta_+(z)^*\left[-\frac{\Delta}{2}\right]\zeta_-(z)dz\right| = \frac{1}{2k_{\min}L_W}\left|\frac{\Delta\sin k_{\min}L_W}{(k_{\min}L_W/\pi)^2-1}\right|. \tag{3.5}$$

This explains the characteristic change shown in Figs. 3 and 4.

Equation (2.3) can be inverted in such a way that the envelope functions at $(z_n^0+z_n^1)/2$ are given by the amplitude $C_0(n)$ and $C_1(n)$. However, the presence of the slight nonparabolicity of the Γ valley gives rise to a deviation from this relation and leads to some errors in estimating the envelope function of X valleys, particularly for states that mainly consist of the Γ valley. A comparison of envelopes calculated in the tight-binding model and in the effective-mass approximation has been made for varying p and the best agreement has been achieved for $0.45\lesssim p\lesssim 0.55$.

Figure 5 gives a comparison of the envelope wave functions of the lowest four bands at $k_x=0$ in $(GaAs)_m(AlAs)_m$ superlattices with $m=16$ for $p=0.5$. The solid line represents the envelope $|\zeta_\Gamma(z)|$ associated with the Γ valley, the dashed line represents $\sqrt{|\zeta_u|^2+|\zeta_v|^2}$ associated with the X valleys, and the symbols represent envelopes obtained in the tight-binding model. The lowest band [Fig. 5(a)] has the character of the Γ valley in the GaAs layer and the higher three bands that of the X valleys. For the lowest band, the envelope associated with the X valleys calculated in the tight-binding model is larger than that of the effective-mass approximation and also shows a different z dependence in the GaAs layer. This discrepancy is due to the nonparabolicity of the Γ valley mentioned above. The envelope function obtained in the effective-mass approximation decays much more rapidly in the AlAs layer for the lowest band as shown in Fig. 5. This is due to the fact that the effective mass inside the band gap of AlAs is much smaller than that at the conduction-band bottom as has been pointed out in a study of the tunneling probability across an $Al_xGa_{1-x}As$ barrier.[1]

Figure 6 gives a similar comparison for $m=13$, for which the lowest two bands have the character of the X valleys. A similar discrepancy can be seen for the second excited band having a Γ-valley character due again to the nonparabolicity of the Γ valley. In spite of such discrepancies, we can safely conclude that the effective-mass calculation can reproduce the wave functions quite well, particularly concerning the strength of the mixing of the Γ and X valleys.

Using the obtained wave functions we can easily estimate the probability of optical transition between the top of the valence and the conduction bands. Figure 2 contains the overlap of the envelope of the lowest conduction-band state and a simple cosine function corresponding to the envelope of the valence-band top. For $m\geq 15$ the conduction-band minimum is comprised mainly of the Γ-valley minimum, and for $m\leq 14$ it is comprised mainly of the X-valley minima. Because of the small mixing between Γ and X, the transition probability for $m\leq 14$ becomes more than two orders of magnitude smaller than that for $m\geq 15$. The parity of the wave function changes with m alternately and gives an oscillation of the probability with m. This oscillation changes

its phase at the thickness where the valley coupling vanishes.

This characteristic parity change is due to the fact that the period for the X-valley Bloch function is two monolayers. This was pointed out by Lu and Sham[10] using group theory and was demonstrated in a tight-binding calculation. Actually, this parity change as a function of m is quite sensitive to $k_{\min}$ and also to whether E_u is smaller or larger than E_v. This oscillatory dependence of the optical transition probability can be used for obtaining detailed information about the conduction-band minima of AlAs near the X points, particularly on the value of $k_{\min}$ and the relative ordering of E_u and E_v.

It may be worthwhile to point out that the obtained value for the parameter p characterizing the mixing between the Γ and X valleys can depend slightly on the model for the bulk band structure of GaAs and AlAs and their interface. In principle, p can be determined by first-principles interface calculations. Unfortunately, this may still give an unreliable answer because of uncertain-

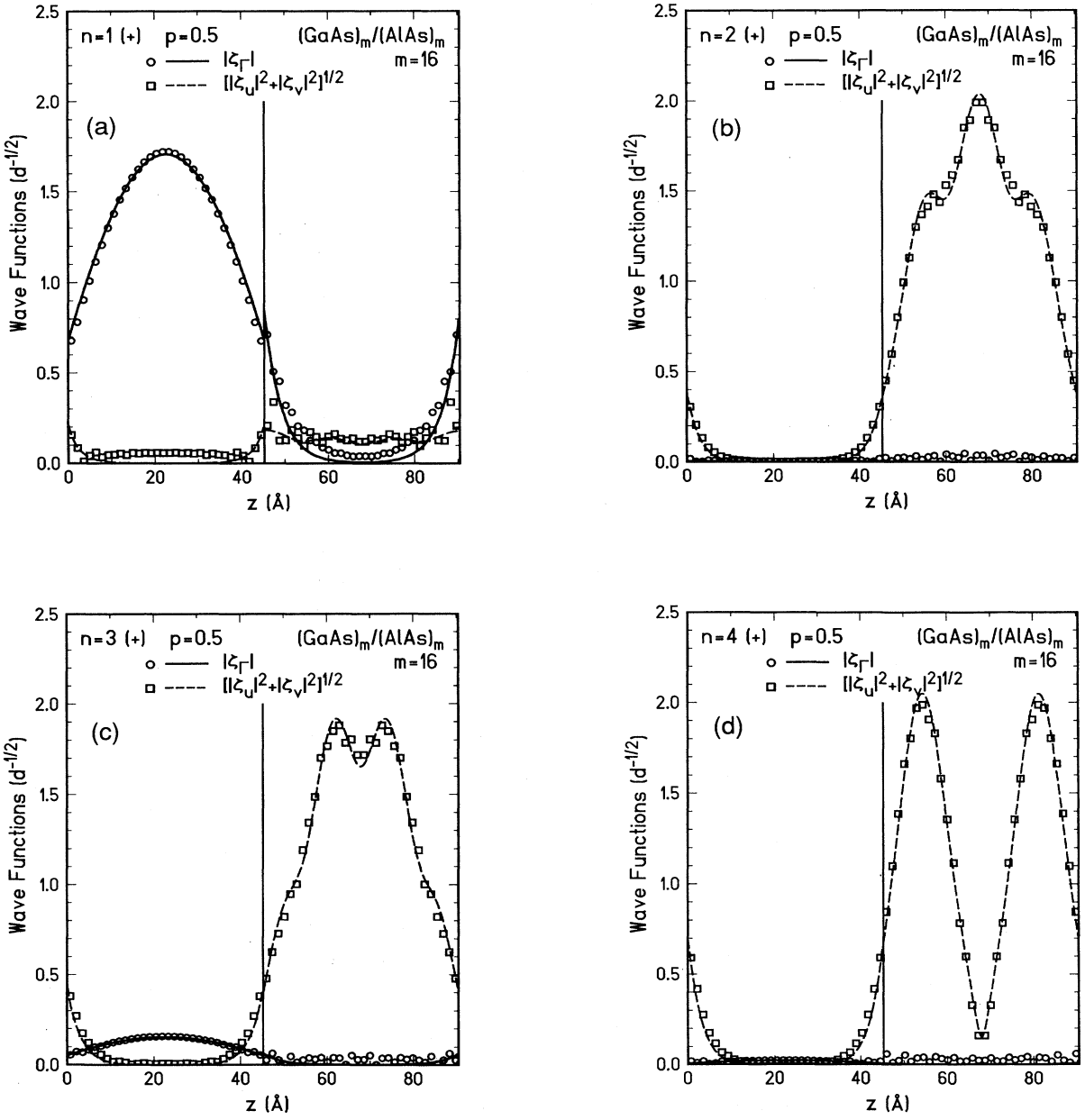

FIG. 5. Envelope functions of the Γ valley (solid lines) and the X valleys (dashed lines) calculated in the effective-mass approximation with valley mixing for mixing parameter $p=0.5$ for the lowest four bands in a $(GaAs)_m(AlAs)_m$ superlattice with $m=16$. Circles and squares represent envelopes for the wave function calculated in the empirical tight-binding model. (a) $n=1$ (the lowest), (b) $n=2$ (first excited), (c) $n=3$ (second excited), and (d) $n=4$ (third excited). The envelope functions are normalized to unity within the superlattice period $d=ma$.

ties present in the band structure near the X points. Therefore, p should be determined rather through comparison with experiments.

IV. SUMMARY AND CONCLUSION

Energy levels and wave functions of short-period GaAs/AlAs superlattices were calculated both in an *sps** tight-binding model and in an effective-mass approximation. Mixing between Γ and X conduction-band valleys was included in the effective-mass approximation through the interface matrix giving boundary conditions for the envelope functions and their derivatives at the interface. The interface matrix was determined in such a way that the flux conservation is satisfied and it reproduces the original result obtained by the direct matching of the wave functions at the interface as much as possible. Two elements giving the strength of Γ-X mixing were obtained by the direct comparison of the wave functions with those calculated in short-period superlattices in an empirical *sps** tight-binding model. The effective-mass approximation together with the appropriate interface matrix can successfully describe the electronic properties of heterostructures.

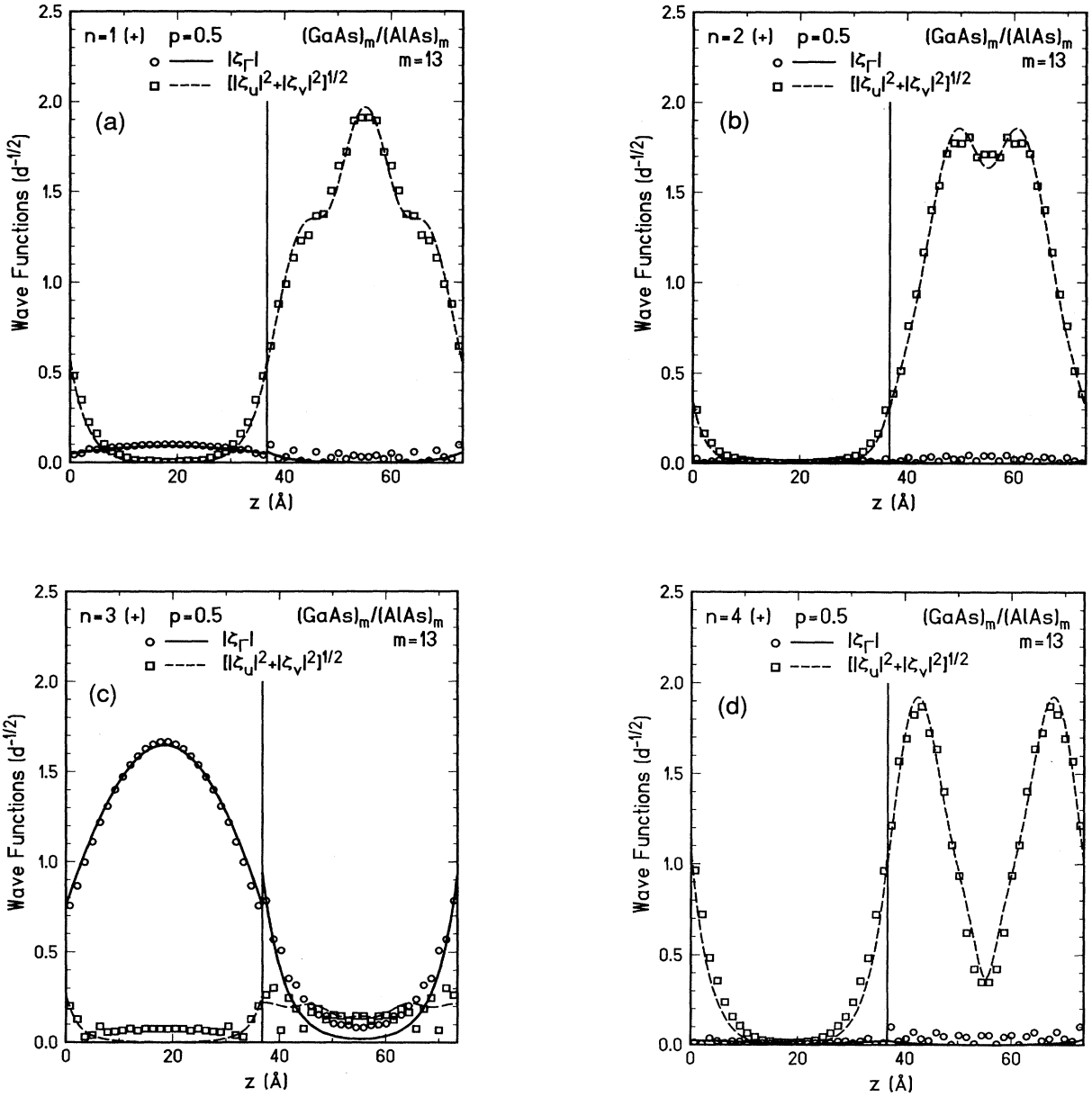

FIG. 6. Envelope functions of the Γ valley (solid lines) and the X valleys (dashed lines) calculated in the effective-mass approximation with valley mixing for mixing parameter $p=0.5$ for the lowest four bands in a $(GaAs)_m(AlAs)_m$ superlattice with $m=13$. Circles and squares represent envelopes for the wave function calculated in the empirical tight-binding model. (a) $n=1$ (the lowest), (b) $n=2$ (first excited), (c) $n=3$ (second excited), and (d) $n=4$ (third excited). The envelope functions are normalized to unity within the superlattice period $d=ma$.

ACKNOWLEDGMENTS

This work was supported in part by the Industry-University Joint Research Program "Mesoscopic Electronics" and by the Grants-in-Aid for Scientific Research on Priority Areas, "Electron Wave Interference Effects in Mesoscopic Structures," and "Computational Physics as a New Frontier in Condensed Matter Research," from the Ministry of Education, Science, and Culture, Japan.

[1]T. Ando and H. Akera, Phys. Rev. B **40**, 11 619 (1989).
[2]See, for example, L. J. Sham and Y.-T. Lu, J. Lumin. **44**, 207 (1989), and references cited therein and in Ref. 3.
[3]T. Ando, S. Wakahara, and H. Akera, Phys. Rev. B **40**, 11 609 (1989).
[4]H. C. Liu, Appl. Phys. Lett. **51**, 1019 (1987); Superlatt. Microstruct. **7**, 35 (1990).
[5]J. B. Xia, Phys. Rev. B **41**, 3117 (1990).
[6]D. Wang, E. A. de Andrada e Silva, and I. C. da Cunha Lima, Phys. Rev. B **46**, 7304 (1992).
[7]H. Kato, Y. Okada, M. Nakayama, and Y. Watanabe, Solid State Commun. **70**, 535 (1989).
[8]M. Nakayama, I. Tanaka, I. Kimura, and H. Nishimura, Jpn. J. Appl. Phys. **29**, 41 (1990).
[9]This was recently pointed out independently by I. L. Aleiner and E. L. Ivchenko, Fiz. Tekh. Poluprovodn. (to be published) [Sov. Phys. Semicond. (to be published)].
[10]Y.-T. Lu and L. J. Sham, Phys. Rev. B **40**, 5567 (1989).